SDC-91-00059

SDC
SOLENOIDAL DETECTOR NOTES

CONVERSION ELECTRONS IN THE SDC

A.B. Wicklund

August 23, 1991

SDC -91-00059
August 23, 1991

Conversion Electrons in the SDC

A. B. Wicklund

We summarize a preliminary analysis of the rates for conversion electrons in the SDC detector, relative to other interesting sources of prompt electrons. We have used Papageno V3.30, and other available NLO calculations to estimate inclusive rates in the central region (η less than 2.0), and we have cross checked these using CDF data at 1.8 TeV. We have considered three sources of "isolated" electrons, namely

(1) Inclusive W/Z production.

(2) Top quark (Mt=140).

(3) QCD prompt photon production, followed by conversion in 10% X0. This value approximates the inner silicon detector at SDC. Additional conversions will occur in the outer tracking chamber, but the trigger and track reconstruction efficiency will be lower.

We have also considered "nonisolated" leptons coming from

(4) Inclusive Bottom production

(5) Photon conversions resulting from π^0, η production in jets.

(6) High Pt hadrons faking electrons.

The efficiency for triggering and reconstructing nonisolated electrons is detector dependent, but we can get an idea of the relative rates for these "electrons" from the CDF data. While the SDC cross sections are typically X10 higher, and harder in Pt, the relative rates for the parton level processes,

(a) W + jet(s)

(b) QCD Photon + jets

(c) b + Jet(s)

(d) $\pi^0 \rightarrow \gamma$, or fake hadron

all scale rather similarly as functions of Pt or Xt.

For process (a), the full NLO calculation (Arnold,Kauffman, Reno) agrees with the CDF Pt(W,Z) distributions at 1.8 TeV; lowest order Papageno (W + 1 jet) gives an adequate

description of these data, provided an overall K=2.2 factor is applied to Papageno. For process (b), we have NLO predictions by Aurenche at 1.8 and 40 TeV, the former in fair agreement with CDF data; the NLO predictions agree with lowest order Papageno (γ + 1 jet), using a K=3 factor. For process (c), the NLO rates predicted by Nason,Ellis,Dawson require a K=3 factor, compared with lowest order Papageno. Figure (1) shows the inclusive electron rates at CDF for $\eta \leq 0.7$, 4.1 pb-1. The electron isolation cuts give an efficiency of 40-50% on the low Pt continuum, which includes bottom electrons (60%), non-identified conversions (18%), and hadron fakes (22%). The W/Z jacobean peak is evident. The total rate for identified conversions, which are removed from fig.1, is approximately 28% of the low Pt continuum in fig. 1. Of the found conversions, we estimate that 30-35% come from QCD prompt photon production, based on their isolation properties. The remaining found conversions are presumably due to π^0, η decays in jets. The nonidentified conversions (18% of the low Pt continuum) are conversion pairs in which the partner positron has low momentum, so that the track reconstruction efficiency is low.

It may seem odd that such a large fraction of found conversions come from QCD prompt photon production, rather than π^0, η decay. The reason is trigger bias. The CDF electron trigger requires a high Pt track in association with a high Et calorimeter deposition, and of course the higher level trigger and offline selection code tightens that requirement. Thus, while a symmetric π^0 decay can satisfy an Et requirement (eg,a "photon trigger"), only asymmetric π^0 decays can give a conversion that satisfies the prompt electron trigger. Figure 2 shows the energy and momentum in a cone of radius 0.7, around prompt electron candidates. The histogram is for identified conversions, while the shaded plot is for other electrons (b-decays, etc), normalized on the right-side of the plot. The quantity plotted is the sum of calorimeter Et and the sum of track momenta, added in quadrature (excluding the electron or conversion pair). The peak at small isolation energy comes from QCD prompt photon production. Figure (3) shows the same distribution for the conversion sample after subtracting the "background" from nonisolated conversions (we use the shaded curve in fig.(2), to describe the background shape.). The histogram shows the same distribution for electrons from W decay, normalized in the first bin. The isolation distributions are evidently quite similar for the "isolated conversions" and the W electrons, provided we exclude the conversion "partner" from the Et,Pt sum.

Figure 4 shows the predicted electron spectra at 1.8 TeV, averaged over ($\eta \leq 2$), from W decay and QCD prompt photons (we use Bethe Heitler to describe the photon conversion to electron pairs, and integrate the total electron rate with no cuts on tagging efficiency.) The solid curve for prompt photons corresponds to 10% X0. The dashed curve is an interpolation of the rate for isolated conversion electrons seen in CDF (the background-subtracted peak in fig.2). We have normalized the observed conversion rate to the W electron peak. The dashed curve is consistent with the solid curve prediction for prompt photons, taking into account the 4.6% X0 equivalent radiator inside the CDF central tracker. Figure 5 shows the same rates for the SDC. Both at CDF and SDC, the prompt photon curve crosses the W$\rightarrow e^{+-}$ curve at around 25 GeV/c Pt. Also shown in fig. 5 is the lowest order T Tbar (Mt=140) rate

from Papageno. We note that the photon predictions are NLO from Aurenche, as described above; the W curve at 1.8 is from the Arnold et al NLO prediction, which agrees with CDF data, and the W curve at 40 TeV is Papageno with a K factor=2.2 . (We have included the Papageno W+0 jet rates with K=1.) We emphasize that the W rates do not include Z→ $e+e-$; to add these, multiply the W rates by 1.2.

Aside from the overall X10 rate increase at the SDC, the W→ $e+-$ curves are similar at the two energies, simply because the electron Pt spectrum is dominated by the jacobean peak in the W → $e\nu$ decay; this peak is smeared more at the higher energy, due to the harder intrinsic Pt(W) spectrum. With a "reasonable" high luminosity trigger, Et> 50,integrated over +-2 units of η, we expect around 2 Hz at 10**33 from W and Top electrons, with 40% conversion background. This may be a reasonable choice for an inclusive single electron trigger, which has been used successfully for virtually all of the heavy flavor and electroweak studies carried out at CDF (CDF used a 12 GeV Et threshold.)

To summarize, the rates for isolated electrons from QCD prompt photons, relative to W→ e+-, Top→e+- etc., are expected to be tolerable with 10% X0 effective radiator in the silicon detector. In particular, the isolated conversions, illustrated in figs. 4,5, should have similar isolation properties (except for the presence of a partner positron) as the electrons from W and Top sources; they should give about half the W→e+- rate for Et≥ 50 GeV. From kinematics, we would expect the conversion finding efficiency to be high (80%), but this needs more detailed simulation. If the conversion identification is well understood, these isolated conversions can be used as a control sample in studies of lepton plus multijet final states (as at CDF.) The isolated conversions are only part of a low Pt continuum, which will include nonisolated conversions, bottom/charm decays, and hadron fakes. If we extrapolate these rates from CDF, assuming the same efficiencies for nonisolated electrons, we predict the following mix for the low Pt (Pt $\leq$ 20) continuum:

		CDF	SDC
(1)	b,c,fakes	64%	47%
(2)	Unseen Conversions	14%	21%
(3)	Seen Conversions	22%	32%
	Total	100%	100%
(4)	Isolated Conversions	11%	16%

The precise mix depends on isolation cuts. We are assuming that the main sources (b production and π^0 decays) scale with Xt as the prompt photon rate. Taking into account the softer Pt spectrum for nonisolated electrons, one would expect this low Pt continuum to extend to the Et≥50 regions in figs. 4,5, with rates comparable to those from isolated conversions.

Figure (6) shows an estimate for the b+bbar inclusive cross section at 40 TeV, averaged over $\eta < 1.5$, based on the Nason, Ellis, Dawson calculation (computation courtesy of R. Meng, priv. comm.). Also shown is the corresponding Pt spectrum for electrons from these b decays, assuming an average 12% b→e B.R.; there is about an order of magnitude reduction

due to the kinematics of b→e decay (eg Pt(e+-) $\ll$ Pt(b)), in addition to the B.R. Using an approximate (CDF based) simulation of the effects of a Had/EM cut, where we require Had/Em<0.04 in a 0.2 X 0.2 Had/EM region, we get the lower curve for "nonisolated" electrons from b-decay. There will be additional acceptance losses associated with overlap of π^0 showers with the electron, but these are not included in this simulation. The acceptance losses associated with a nominal Had/EM cut become quite severe for Pt(e+-) > 20 GeV/c, due to the hadronic fragments accompanying the electron (note that the B-meson mass and the transverse size of the hadron jet are fixed.) The actual inclusive b-quark cross section at SDC may be significantly higher than the NSD calculation (CDF observes 2.4X the NSD rate). In general, as expected the b-rates are comparable to those for conversion electrons, depending on the actual enhancement over QCD.

Figure Captions

1. Inclusive electron spectrum from CDF; dahsed curve shows expected charm contribution, solid shows bottom+charm . Crosses denote electron rates with W,Z electrons subtracted.

2. Isolation distribution for conversion electrons in CDF (total histogram), and for prompt electrons (shaded region.)

3. Isolation distribution for conversion electrons in CDF, using prompt electrons to provide background subtraction shape (points), and isolation distribution for W electrons (histogram.)

4. Predicted electron rates at CDF from W decay and from prompt photon conversions with 10% X0. Dashed curve shows observed CDF rate for 4.6 % X0.

5. Same as (4) for 40 TeV, including Top(M=140) contribution.

6. Inclusive rates for bottom quark (b plus bbar) production in $\eta \leq 1.5$, and for prompt e+- from b-quark decay with no efficiency cuts (top curve) and with expected Had/Em cut (bottom curve.) Electron rates include 12% semileptonic B.R.

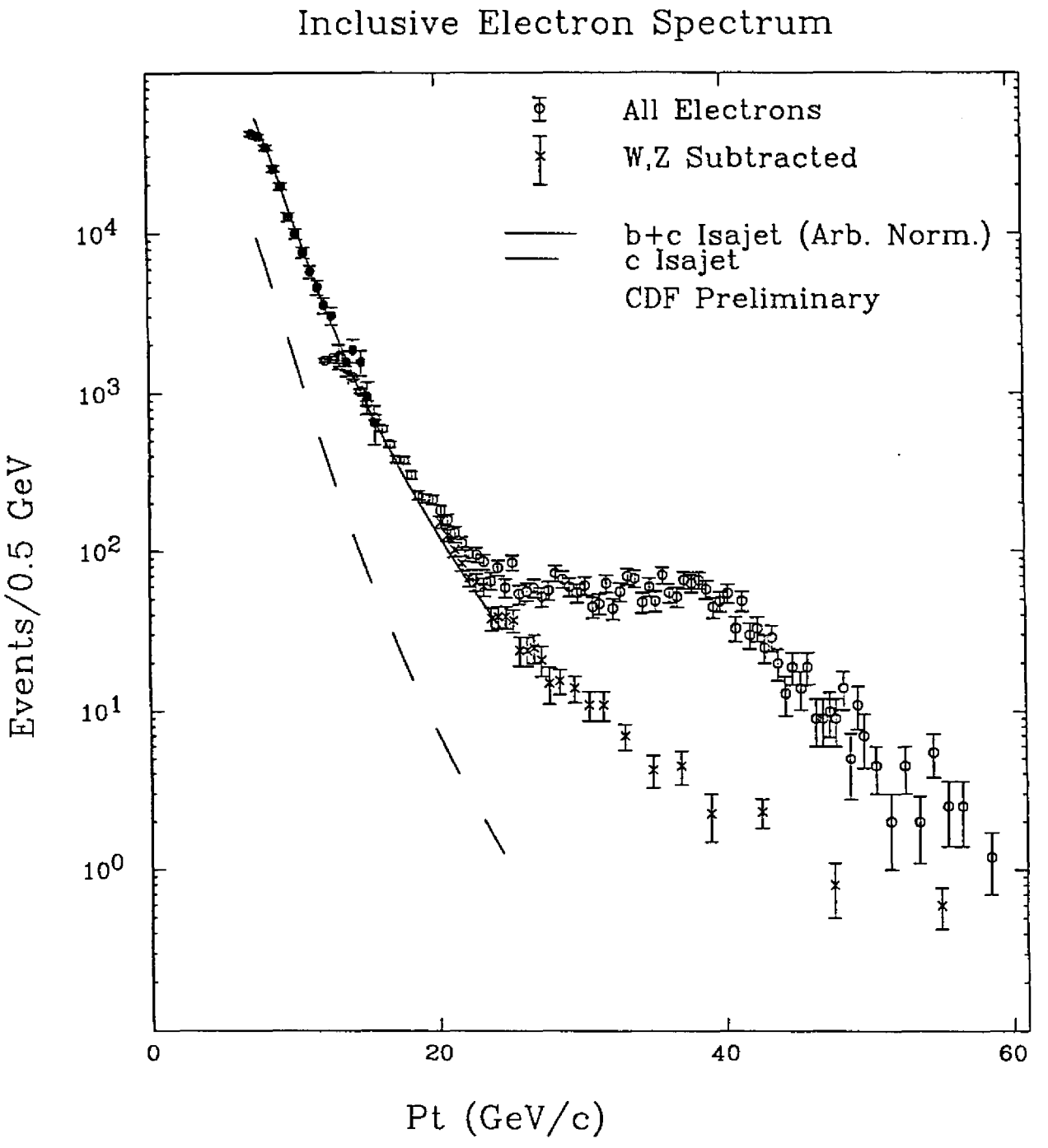
Inclusive Electron Spectrum
All Electrons
W,Z Subtracted
b+c Isajet (Arb. Norm.)
c Isajet
CDF Preliminary
Events/0.5 GeV
10^4
10^3
10^2
10^1
10^0
0
20
40
60
Pt (GeV/c)

(Fig. 1)

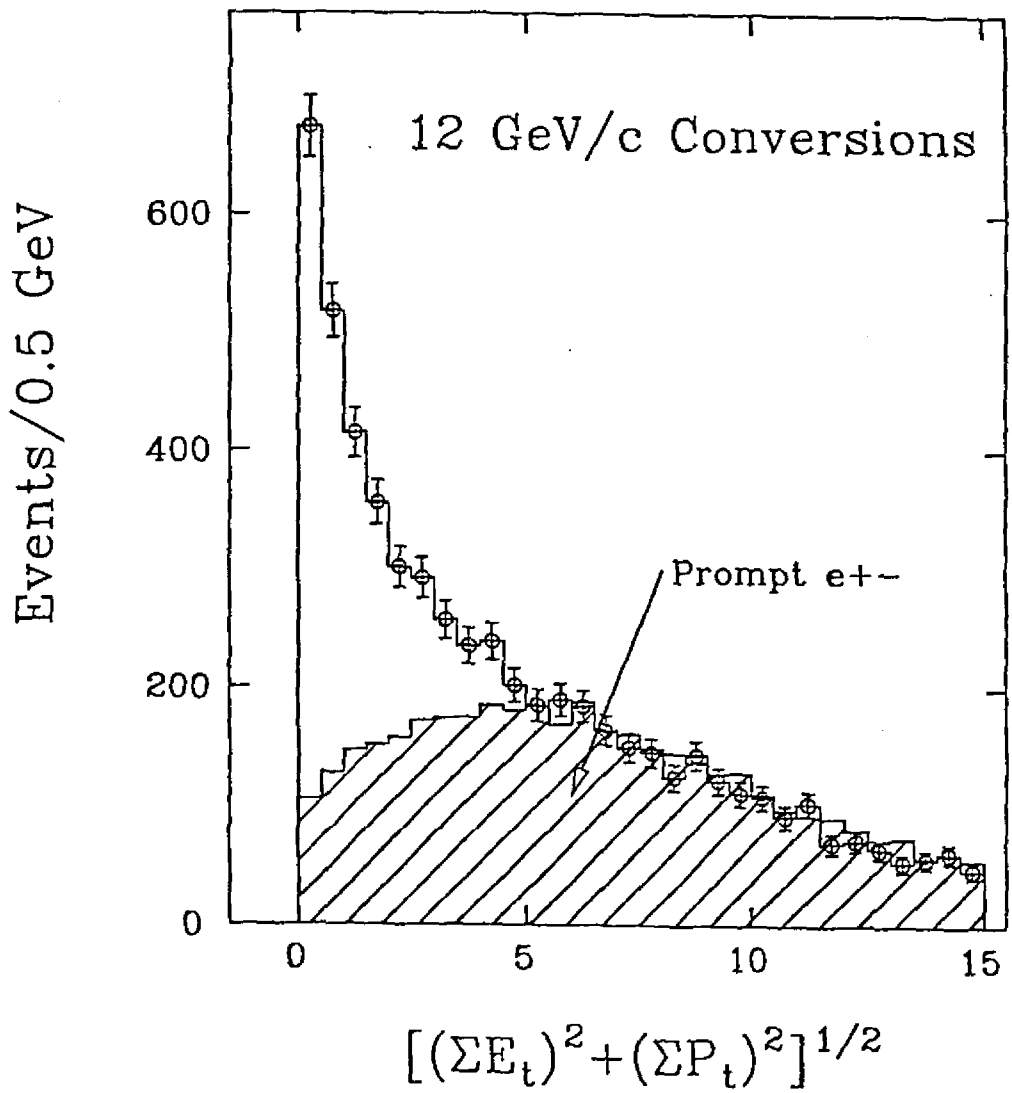
12 GeV/c Conversions
Events/0.5 GeV
600
400
200
0
Prompt e+-
0
5
10
15
$[(\Sigma E_t)^2+(\Sigma P_t)^2]^{1/2}$

Fig. (2)

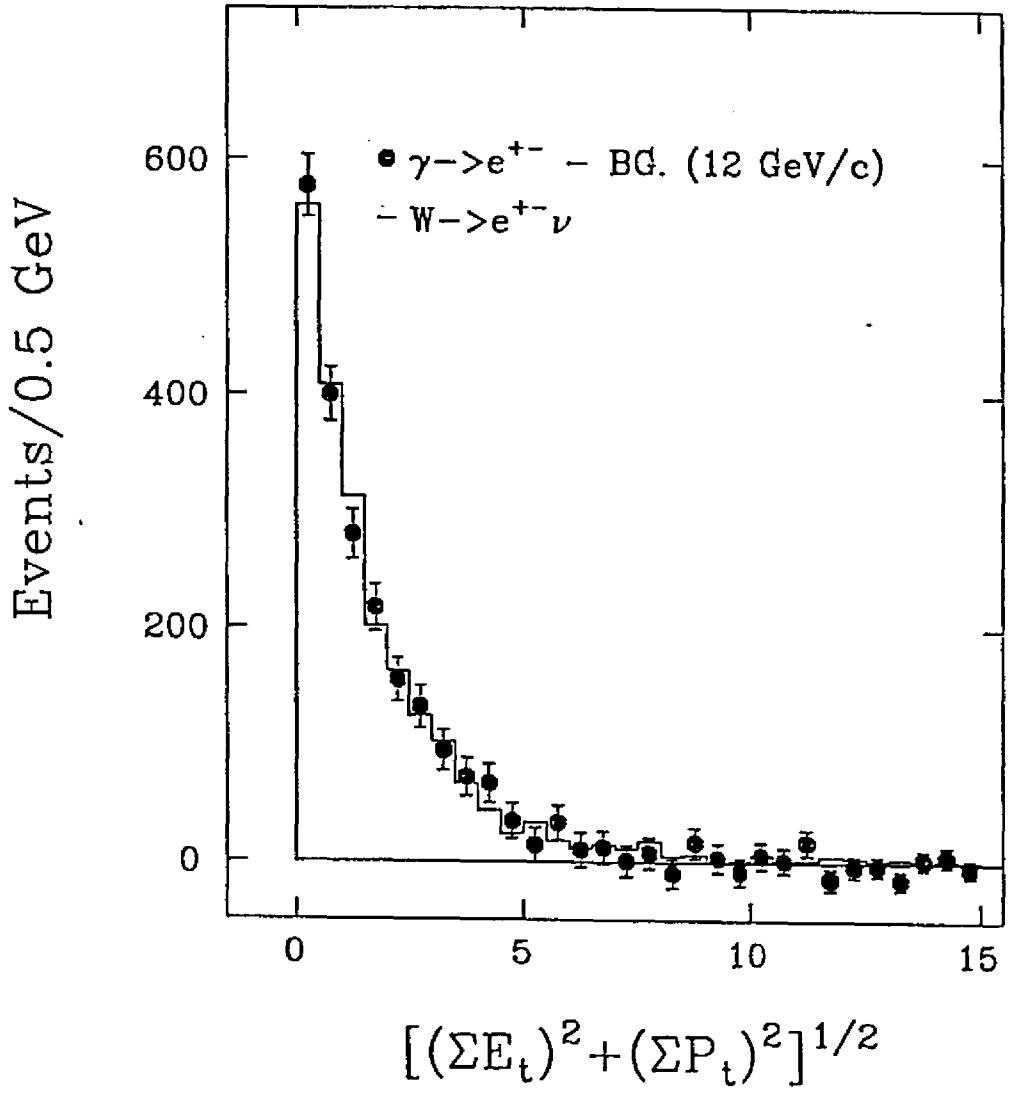
Events/0.5 GeV
600
400
200
0
0
5
10
15
γ->e+- - BG. (12 GeV/c)
- W->e+-ν
[(ΣEt)2+(ΣPt)2]1/2

Fig. (3)

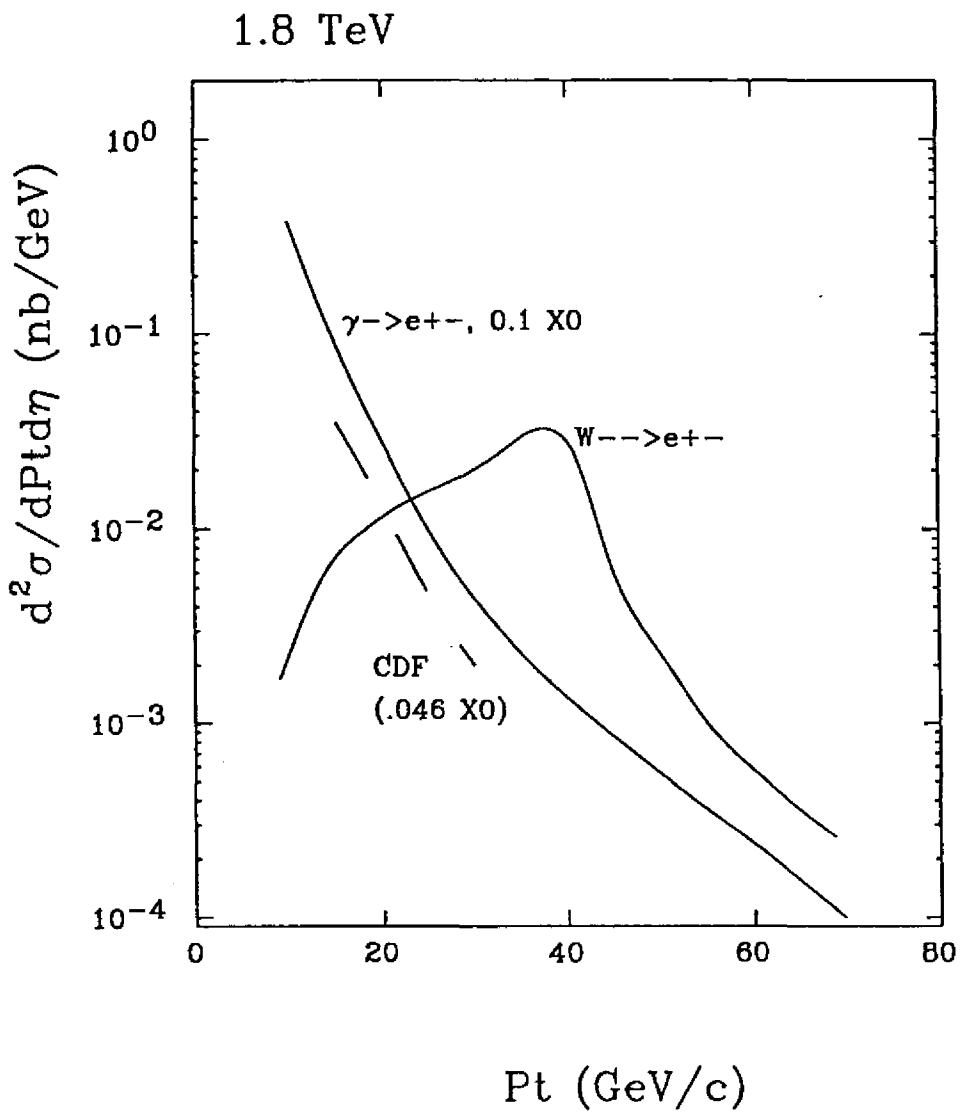
1.8 TeV
$d^2\sigma/dPtd\eta$ (nb/GeV)
10^0
10^{-1}
10^{-2}
10^{-3}
10^{-4}
γ->e+-, 0.1 X0
W-->e+-
CDF
(.046 X0)
0
20
40
60
80
Pt (GeV/c)

(Fig. 4)

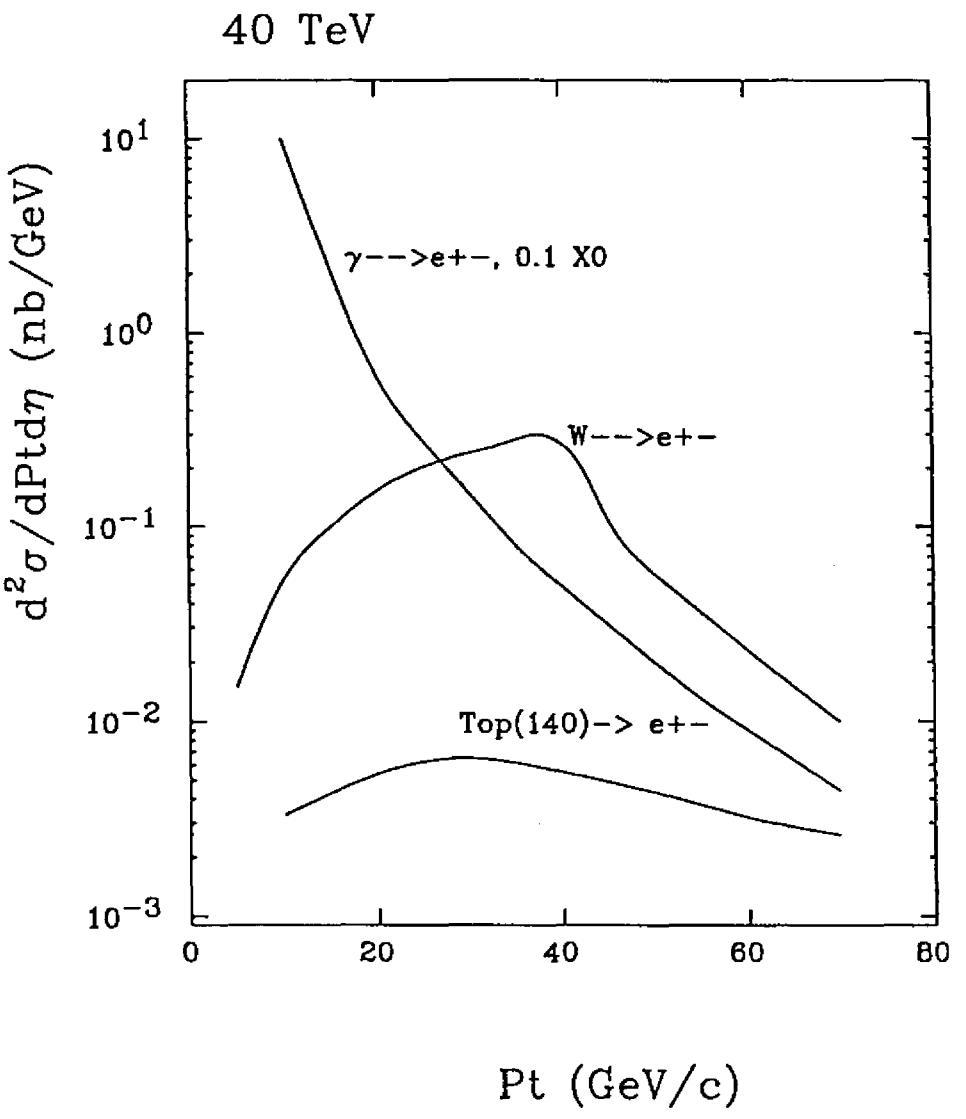
40 TeV
$d^2\sigma/dPtd\eta$ (nb/GeV)
10^1
10^0
10^{-1}
10^{-2}
10^{-3}
γ-->e+-, 0.1 X0
W-->e+-
Top(140)-> e+-
0
20
40
60
80
Pt (GeV/c)

(Fig. 5)

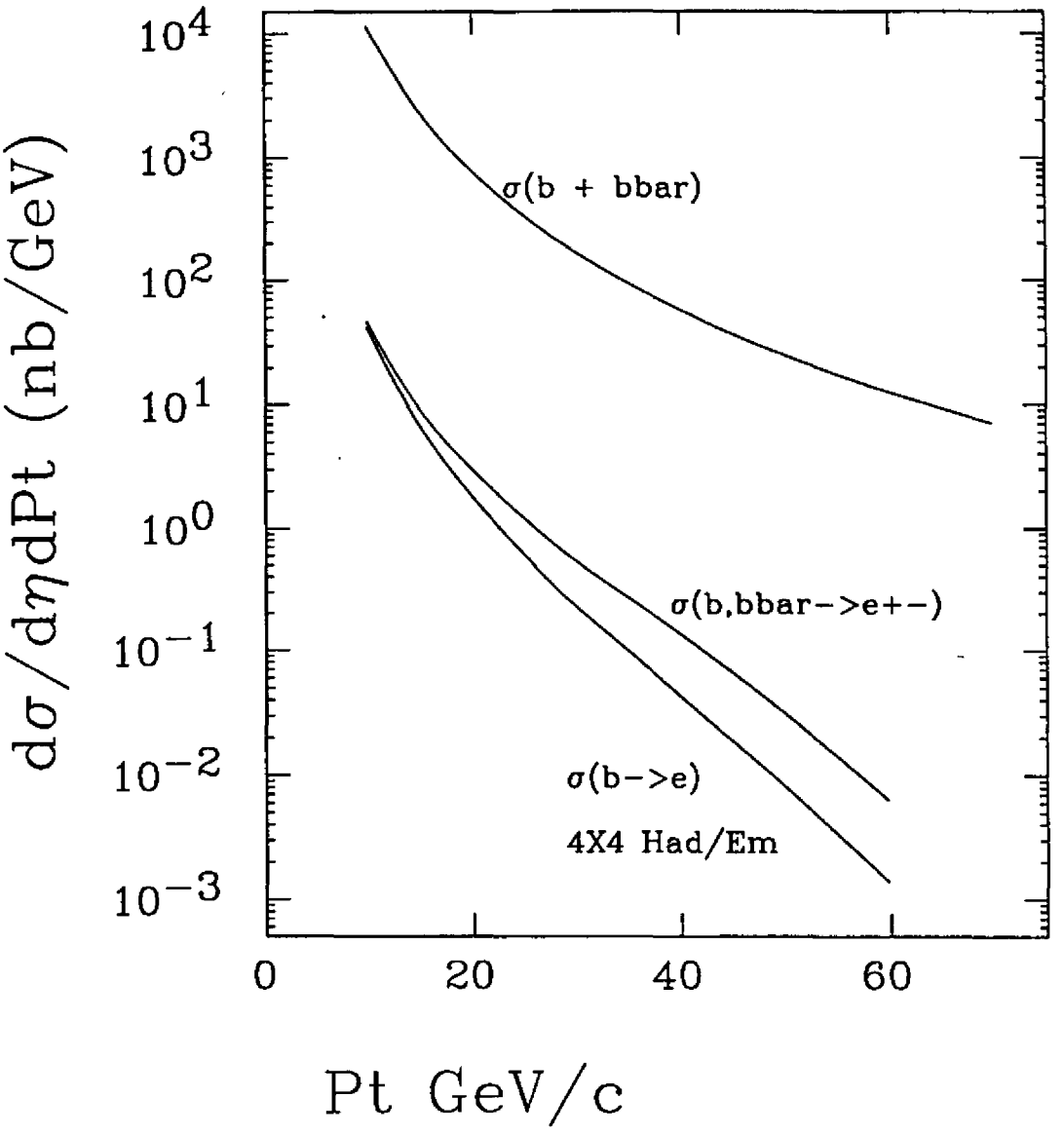
10^4
10^3
10^2
10^1
10^0
10^{-1}
10^{-2}
10^{-3}
$d\sigma/d\eta dPt$ (nb/GeV)
σ(b + bbar)
σ(b,bbar->e+-)
σ(b->e)
4X4 Had/Em
0
20
40
60
Pt GeV/c

Fig (6)